IEEE Photonics Journal
An IEEE Photonics Society Publication

Investigation of Underwater Wireless Optical Communications Links With Surface Currents and Tides for Oceanic Signal Transmission

Volume 13, Number 3, June 2021

Zhijian Lv
Gui He
Chengfeng Qiu
Zhaojun Liu, ***Senior Member, IEEE***

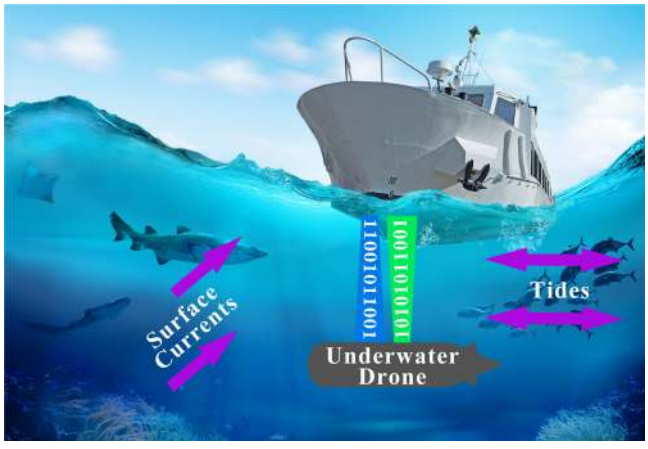

DOI: 10.1109/JPHOT.2021.3076895

IEEE photonics SOCIETY
IEEE

Investigation of Underwater Wireless Optical Communications Links With Surface Currents and Tides for Oceanic Signal Transmission

Zhijian Lv, Gui He, Chengfeng Qiu, and Zhaojun Liu, *Senior Member, IEEE*

Department of Electrical and Computer Engineering, Southern University of Science and Technology, Shenzhen 518055, China

DOI:10.1109/JPHOT.2021.3076895

Manuscript received March 28, 2021; revised April 22, 2021; accepted April 28, 2021. Date of publication April 30, 2021; date of current version July 30, 2021. This work was supported in part by Shenzhen Science and Technology Program under Grant KQTD20170810110313773, in part by Shenzhen Science and Technology Program under Grant JCYJ20190812141803608, in part by Special Funds for the Cultivation of Guangdong College Students' Scientific and Technological Innovation ("Climbing Program" Special Funds, Project Pdjh2020b0521), in part by Key-Area Research and Development Program of Guangdong Province under Grant 2019B010925001, in part by Shenzhen Overseas High-level Talent Innovation Team (Project Name: Micro-LED Displays Technology and Demonstration Innovation Team for Novel VR/AR Applications, under Grant KQTD201708101103-13 773), and in part by Guangdong Science and Technology Funding (Project Name: High Speed Visible Light Communications based on RGB Micro-LED Arrays, under Grant 2017B010114002). Corresponding author: Zhaojun Liu. (e-mail: liuzj@sustech.edu.cn).

Abstract: This report investigated underwater wireless optical communication (UWOC) links in the presence of surface currents and tides. The scenario of surface currents and tides was generated by a sea water tank, a water pipe, and a water pump of different flow rates. It built the oceanic channel of UWOC varied with the salinity and flow rate in the UWOC transmission. The data rate of UWOC links based on a 520-nm laser diode and none-return-to-zero on-off keying (NRZ-OOK) modulation can achieve 3.4 Gb/s at a bit error rate (BER) of 3.78 $\times 10^{-4}$ in 1.8 m long sea water tank when a flow rate reached 1.08 m/s. The BER, eye-diagrams, and received signal optical power measurements showed that both the increasing salinity and flow rate cause the UWOC channel attenuation, thus degrade the performance of UWOC links.

Index Terms: Underwater wireless optical communications, turbulence.

1. Introduction

Demands for high speed, large bandwidth underwater data communication links are growing to meet the explosive underwater human activities. Underwater ultrasound communication is limited to the narrow bandwidth, which works at a low data rate of tens of kb/s over a range of km. Underwater radio frequency (RF) communication is limited to the range of shorter than 10 m because of the high attenuation in the sea. Compared to them, underwater wireless optical communication (UWOC) links based on laser diodes (LDs) can balance a high data rate up to Gb/s and a moderate transmission range of 100 m [1]–[13]. Recently, UWOC has attracted significant attention as a

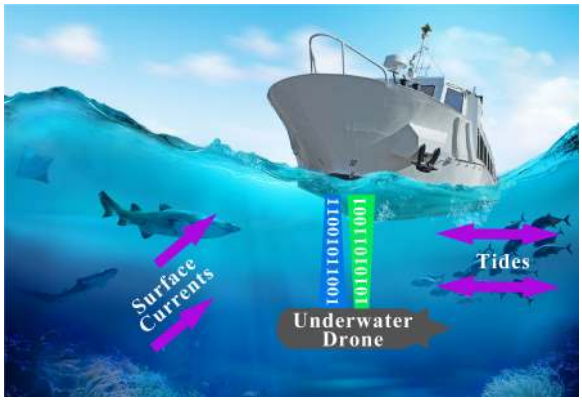

Fig. 1. Illustration of surface currents and tides interactions to the UWOC links between the ship and the underwater drone.

solution to high-speed moderate-range underwater communication for ocean study, offshore oil expedition, and aquaculture.

The performance of UWOC links is highly correlated to three key factors including scattering, absorption, and turbulence. Underwater optical scattering is due to the light beam diffused from the initial path when the particles and bubbles are floating in the water. In underwater optical absorption, the optical path loss results from the water molecules, the salinity, and other particles. Underwater optical turbulence occurs due to the random variations of the refraction index along the optical path that could arise due to the presence of dissolved and suspended particles in the water. It is impacted by the uniformity changed by the water flow. The recent UWOC studies have paid more attention to the effects of absorption and scattering generated by particles and bubbles in the UWOC channel. In 2017, Oubei *et al.* from KAUST evaluated the performance of underwater wireless optical communications links in the presence of different air bubble populations [14]. In 2019, Tian *et al.* from Fudan University announced the research on absorption and scattering effects of maalox, chlorophyll, and sea salt on a micro-LED-based underwater wireless optical communication [15]. Meanwhile, Xu *et al.* from USTC investigated the effects of air bubbles on underwater optical wireless communication [16].

However, there is little UWOC research on the turbulent effects of water flow [17]–[21]. Surface currents and tides are common phenomena in the sea, which cause the motion of sediments and bubbles. Furthermore, the North Pacific Current or the North and South Equatorial currents travel at speed of 0.03 to 0.06 m/s. The Gulf Stream, and the Kuroshio Currents flow with speed up to 0.4 to 1.2 m/s. California Currents and the Canary Current travel at 0.03 to 0.07 m/s. Therefore, the velocity range is set between 0.7 m/s and 1.08 m/s [22].

In the lab, we firstly established an oceanic channel of UWOC varied with the salinity and flow rate. Its turbulence exerted a negative impact on the performance of UWOC links owing to the degradation of received signal optical power as shown in Fig. 1. Therefore, the investigation of UWOC links in the presence of surface currents and tides becomes significant, which could build a more practical scenario of UWOC links in the sea.

2. Experimental Details

Fig. 2 shows the schematic of the experimental setup for UWOC measurements using a 520-nm LD and none-return-to-zero on-off keying (NRZ-OOK) modulation scheme. At the transmitter side, a TO-56 packaged single-mode green LD (Osram PLT5 520) with a collimation lens was mounted on a thermoelectric cooler (TEC) module (SaNoor SN-LDM-T-P). The LD was performed at room temperature. The pattern generator in the J-BERT (Agilent N4903 A) was used to generate the pseudorandom binary sequence (PRBS) 2^{23}-1 pattern as digital input signal. A direct current (DC)

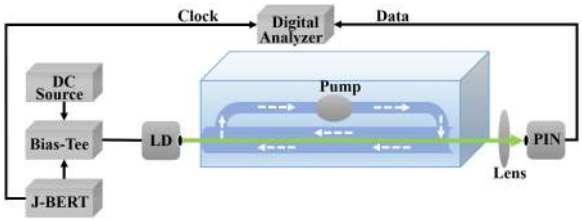

Fig. 2. Schematic of the experimental setup for laser based underwater optical wireless communications measurements.

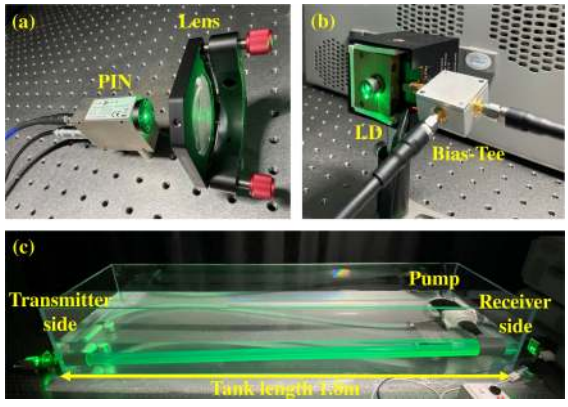

Fig. 3. Images of the 520-nm LD-based UWOC: (a) the PIN receiver and Lens, (b) the packaged LD and the Bias-Tee, (c) the communication channel based on the LD UWOC with sea water in the tank.

bias (SaNoor Laser Driver-5 A) was added to the digital input signal by a Bias-Tee (Mini-Circuits ZFBT-6GW) driving the green LD. At the receiver side, a convex lens (DHC GCM-0858850 M) was used to focus the light into the PIN receiver (FEMTO HAS-X-S-1G4-SI-FS). The eye diagram was collected using a digital communications analyzer (Agilent 86100A & HP 83483A). The bit error rate (BER) and data rate were measured using J-BERT (Agilent N4903 A). A parametric network analyzer (ROHDE & SCHWARZ Vector Network Analyzer ZVB 8) was used for the small-signal bandwidth measurement. The LD characterization setup involved a precision source meter (Keysight B2902A) and optical power monitor (Thorlabs PM100D) for the voltage vs. current and optical power vs. current measurement. The water tank in this research was filled with tap water or sea water at a salinity of 35.42 g/L. The circulation in the tank was built up with the sea water, a water pipe, and a water pump of different flow rates between 0.7 m/s and 1.08 m/s. The flow rate was measured along the optical link in the pipe, which was the effective flow rate. In addition, it was uniform in this measurement. Thus, it brought the turbulent effect into the UWOC channel. Fig. 3(a) shows the images of the PIN receiver and the lens at the receiver side. Fig. 3(b) illustrates the images of the packaged 520-nm LD with a collimation lens and the Bias-Tee at the transmitter side. Fig. 3(c) demonstrates the UWOC channel in the sea water tank of dimensions 1.8 m $\times$ 0.8 m $\times$ 0.5 m. The circulation includes a pipe and a pump to generate the turbulent effect in the sea water tank.

3. Results

The optical power-current-voltage (LIV) characteristics of 520-nm LD is shown in Fig. 4(a). The threshold current is 50 mA when the corresponding voltage is 4.56 V. At the forward current of 110 mA, the LD has an optical output power of 30.1 mW in free space. Through 1.8 m long tap water tank, the received optical power decreases to 20.2 mW with an attenuation of 33%. Within 1.8 m long sea water tank at a salinity of 35.42 g/L, the received optical power degrades to 2.71 mW

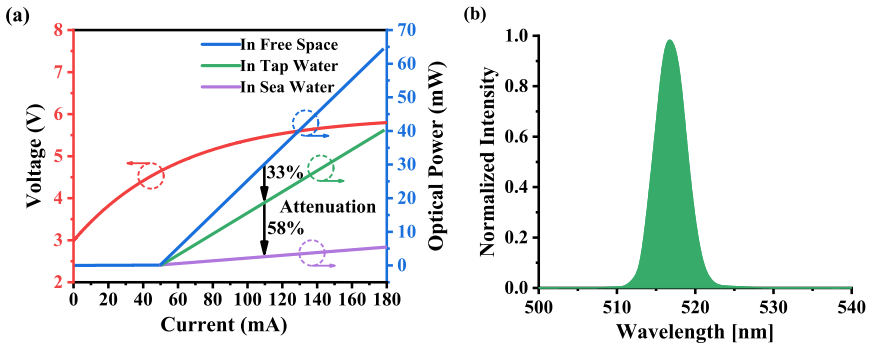

Fig. 4. (a) Voltage vs. current and optical power vs. current characteristics of the laser diode with free space, tap water, and sea water. (b) Normalized intensity vs. wavelength of the laser diode.

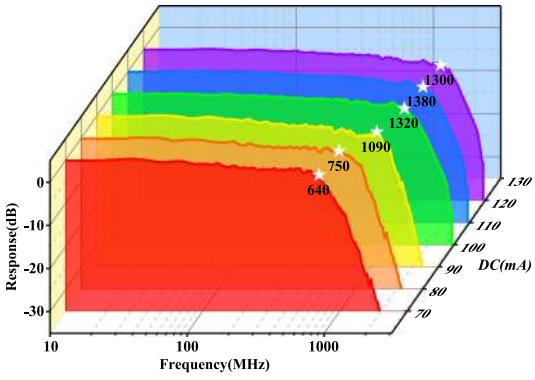

Fig. 5. Frequency response of the system at different bias currents. It indicates the -3 dB bandwidth of UWOC links is 1.3 GHz.

with an attenuation of 91%. When a small signal is modulated to the direct current, it would result in the optical power variation of the LD. Because the L-I plot with tap water or sea water presents a linear relationship, the green LD is a good transmitter candidate for UWOC. Fig. 4(b) shows the LD emits the light at the wavelength of 520 nm. There is no optical intensity beyond the range from 510 nm to 525 nm. As shown in Fig. 5, the normalized frequency response of UWOC links is measured in 1.8 m long sea water tank at different bias current. When bias current increases from 100 mA to 120 mA, the 3-dB system bandwidth keeps constant approximately at 1.3 GHz because the bandwidth of the commercial PIN photo receiver is limited to 1.3 GHz. In addition, the frequency response of UWOC links drops rapidly after the 3-dB bandwidth frequency.

In UWOC links, the optimal operating point of UWOC links is captured from Fig. 6(a) and (b). The UWOC links work at a data rate of 3.3 Gb/s. The typical forward current of 520-nm LD is 110 mA from the data sheet. We set DC bias current to 110 mA as the original operating point in order to obtain the modulation voltage. When the modulation voltage increases from 0.2 V to 0.5 V, the BER decreases gradually from 2.89×10^{-4} to 3.39×10^{-5}. When the modulation voltage continues to go up from 0.5 V to 0.8 V, the BER becomes worse to 8.06×10^{-5}. Thus, the optimal modulation voltage at 110 mA DC bias current is 0.5 V. On the other hand, we set the modulation voltage to 0.5 V as the optimal operating point. When the DC bias current increases from 85 mA to 110 mA, the BER goes down from 2.7×10^{-4} to 3.39×10^{-5}. When the DC bias current keeps increasing to 135 mA, the BER turns to 4.71×10^{-4}. Therefore, 110 mA DC bias current and 0.5 V modulation voltage is the optimal operating point of the presented UWOC links.

Using the Rytov theory, Korotkova and coworkers have evaluated the scintillation index of an optical plane and spherical waves in a weak turbulent water channel. The bit error rate (BER)

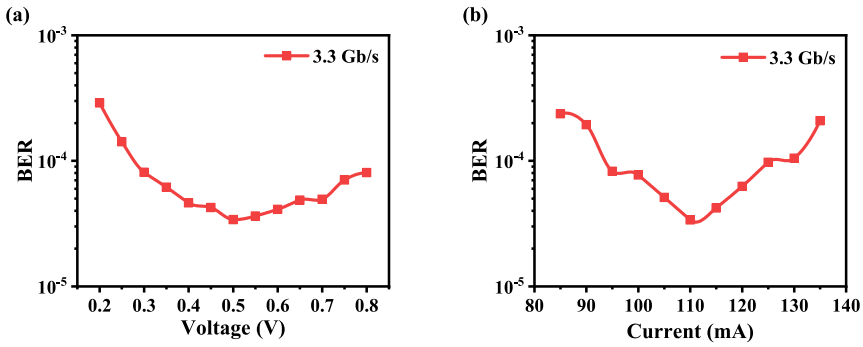

Fig. 6. (a) The optimization of BER for different modulation voltages when DC bias current is 110 mA at a data rate of 3.3 Gb/s. (b) the optimization of BER for DC bias currents when modulation voltage is 0.5 V at a data rate of 3.3 Gb/s.

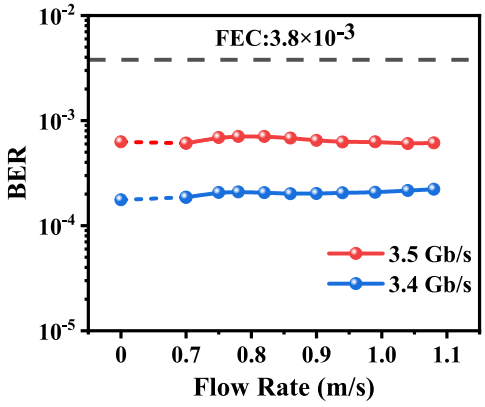

Fig. 7. BERs with data rates of 3.4 Gb/s and 3.5 Gb/s with tap water in the tank at different flow rates. It indicates that the tap water flow can not impact the performance of UWOC links much.

performance of UWOC systems with a log-normal distribution as a channel fading model and the BER of focused Gaussian beams in weak turbulence were investigated [23]–[28].

Based on the turbulent theory, we chose the BER as the key factor to evaluate the weak turbulent effect. As a control experiment, we established the UWOC link in the tap water tank by using a 520-nm LD and OOK modulation scheme. It can transmit at the highest data rate of 3.5 Gb/s under the feed forward error correction (FEC) limit of 3.8×10^{-3} when the DC bias current was 110 mA and the modulation voltage was 0.5 V. As shown in Fig. 7, we chose the date rates of 3.4 Gb/s, and 3.5 Gb/s to investigate the oceanic turbulent effect in the UWOC links. The circulation in the water tank included a pipe with a diameter of 42 mm and a pump varied with different flow rates between 0.7 m/s and 1.08 m/s to simulate the Gulf Stream velocity. Under the condition of tap water underwater channel, even if the pump was turned on to the highest speed, the received optical power decreased slightly from 20.2 mW to 17 mW without the collecting lens at the receiver side. Although the signal-noise-ratio (SNR) of UWOC links became worse, the received optical power was high enough that the PIN photo receiver was in the saturation mode. Therefore, the BER of UWOC links kept stable at 2×10^{-4} with a data rate of 3.4 Gb/s, and 6×10^{-4} with a data rate of 3.5 Gb/s. To conclude, the oceanic turbulence does not exert a significant impact on the UWOC links under tap water condition.

To enhance the turbulent effect in the UWOC links, we attempted to add the factor of sea salt in the water tank to build the sea water scenario. 500 g sea salt was added into 120 L tap water in the water tank per time. Thus, the sea salt concentration increased by 4.17 g/L for each step. The DC bias current and the modulation voltage were the same as those under tap water condition.

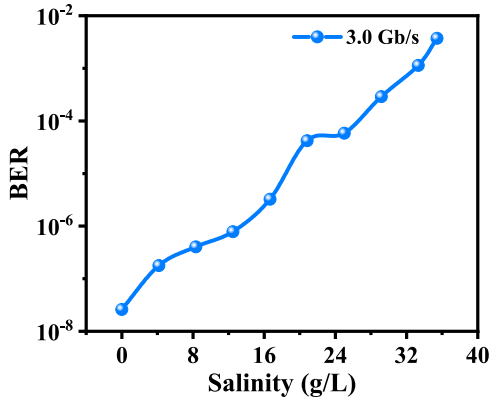

Fig. 8. Variation of BERs with data rates of 3.0 Gb/s for different sea salt concentrations.

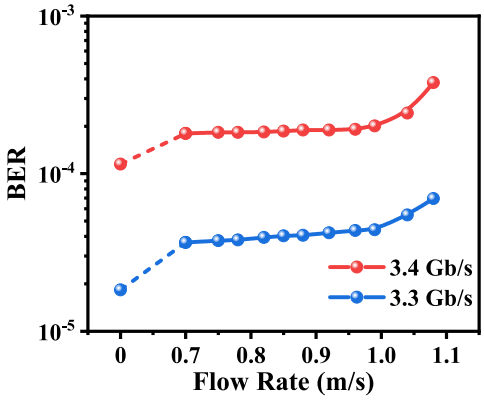

Fig. 9. BERs with data rates of 3.3 Gb/s and 3.4 Gb/s with sea water in the tank at different flow rates. It indicates that the tap water flow can not impact the performance of UWOC links much.

As shown in Fig. 8, when the salinity increased from 0 to the sea water concentration 35.4 g/L, the absorption of sea water in UWOC links increased rapidly degrading the received optical power from 20.2 mW to 2.71 mW. The highest data rate we can achieve with sea water tank under the FEC limit was 3 Gb/s without the collecting lens at the receiver side. The BER at a data rate of 3.0 Gb/s also degraded from 2.6×10^{-8} to 3.7×10^{-3}.

To further confirm the relationship among the salinity, the flow rate, and the UWOC links performance, we chose the salinity of 35.4 g/L as same as the sea water and adjusted the power of the pump for different flow rates. The DC bias current and the modulation voltage were the same as the optimal point discussed above. As shown in Fig. 9, when the pump started for a flow rate of 0.7 m/s, the received optical power decreased sharply from 2.71 mW via the standing water to 1.2 mW via the flowing water. The BER of UWOC links increased dramatically from 1.15×10^{-4} to 1.80×10^{-4} at a data rate of 3.4 Gb/s. With the flow rate increasing to 1.08 m/s, the received optical power reduced to 0.8 mW. The BER of UWOC links also became worse to 3.78×10^{-4} slightly. The received optical power was scintillating due to the turbulent effect. We had to add the collecting lens at the receiver side in this experiment. Without the collecting lens, the PIN photo receiver can not detect the signal from the background noise. When the UWOC links were affected by the turbulent effect in the sea water tank with data rates of 3.3 Gb/s, the corresponding BER performances showed similar trends to that of 3.4 Gb/s.

The eye diagrams were captured by a 14 GHz digital oscilloscope (Aglient 86100 A). Fig. 10(a) (b) (c) show the eye diagrams with data rates of 2.5 Gb/s, 3.0 Gb/s, and 3.4 Gb/s in standing sea water. Fig. 10 (d) (e) (f) demonstrate the eye diagrams with data rates of 2.5 Gb/s, 3.0 Gb/s, and

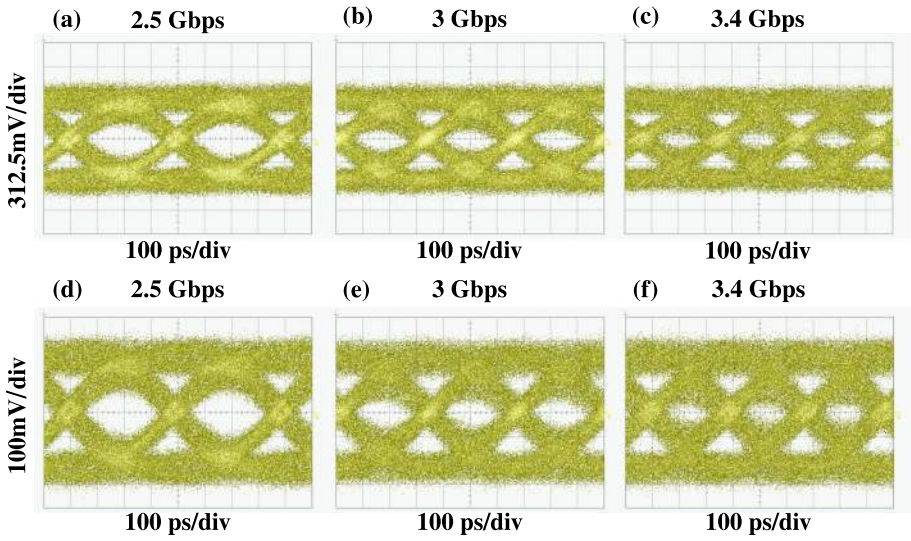

Fig. 10. (a) (b) (c) Eye diagrams with data rates of 2.5 Gb/s, 3 Gb/s, and 3.4 Gb/s with sea water in the tank without flow rate. (d) (e) (f) Eye diagrams with data rates of 2.5 Gb/s, 3 Gb/s, and 3.4 Gb/s with sea water in the tank with a flow rate of 1.08 m/s.

TABLE 1
Key Parameters Corresponding to the Eye Diagrams

Flow rate (m/s)	Data rate (Gb/s)	Rising time (ps)	Falling time (ps)	SNR	Jitter RMS (ps)	BER
0	2.5	308.9	277.8	3.84	27.85	0
0	3	246.7	235.6	2.92	32.44	2.65×10^{-6}
0	3.4	146.7	188.9	2.27	37.38	1.15×10^{-4}
1.08	2.5	324.4	333.3	3.7	30.58	0
1.08	3	240	224.4	2.77	33.37	5.68×10^{-6}
1.08	3.4	137.8	106.7	2.23	43.96	3.78×10^{-4}

3.4 Gb/s in flowing sea water at a flow rate of 1.08 m/s. Table 1 shows key parameters corresponding to the eye diagrams including data rate, rising time, falling time, SNR, jitter root-mean-square (RMS), and BER. Compared two sets of eye diagrams, the eye heights with sea water in the tank without flow rate are higher. It indicates that the SNR of the standing sea water is much higher than that of the flowing sea water at various flow rates owing to the turbulent effect. In conclusion, the salinity-induced oceanic turbulence exerts a significant effect to the UWOC links. In further study, we will analyze other factors that induce the oceanic turbulence, such as temperature gradients, pressure, air bubbles, and so on.

4. Conclusion

In this paper, we firstly experimentally demonstrated the salinity and flow rate induced turbulence employing to the high-speed UWOC links by using 520-nm LD and OOK modulation scheme. The circulation in the 1.8 m long sea water tank includes a pipe and a pump varied with flow rates to build the oceanic turbulence. The theoretical analysis indicates that both BER and SNR performance of UWOC links have a strong relationship with the salinity-induced turbulent effect varied with flow rates. Furthermore, the experiment shows in the tap water the weak turbulence by flow rate exerts a little impact on the performance of UWOC links. But the increasing salinity and flow rate result in the scintillation via UWOC channel, degrading the performance of UWOC links rapidly.

Acknowledgment

The authors wish to thank Prof. Hao-Chung Kuo, Ke Zhang, and Lijiang Huang for their valuable suggestions and support. The authors would also like to thank Chiao Tung University, Hong Kong University of Science and Technology, and Shenzhen Sitan Technology Company Ltd.

References

[1] Y.-F. Huang, C.-T. Tsai, Y.-C. Chi, D.-W. Huang, and G.-R. Lin, "Filtered multicarrier OFDM encoding on blue laser diode for 14.8-Gbps seawater transmission," *J. Lightw. Technol.*, vol. 36, no. 9, pp. 1739–1745, 2017.
[2] T.-C. Wu, Y.-C. Chi, H.-Y. Wang, C.-T. Tsai, and G.-R. Lin, "Blue laser diode enables underwater communication at 12.4 Gbps," *Sci. Reports*, vol. 7, no. 1, pp. 1–10, 2017.
[3] Y.-C. Chi, D.-H. Hsieh, C.-T. Tsai, H.-Y. Chen, H.-C. Kuo, and G.-R. Lin, "450-nm gan laser diode enables high-speed visible light communication with 9-Gbps qam-ofdm," *Opt. Exp.*, vol. 23, no. 10, pp. 13051–13059, 2015.
[4] H. Kaushal and G. Kaddoum, "Underwater optical wireless communication," *IEEE Access*, vol. 4, pp. 1518–1547, 2016.
[5] Z. Zeng, S. Fu, H. Zhang, Y. Dong, and J. Cheng, "A survey of underwater optical wireless communications," *IEEE Commun Surveys Tuts.*, vol. 19, no. 1, pp. 204–238, Oct.–Dec, 2017.
[6] X. Sun *et al.*, "A review on practical considerations and solutions in underwater wireless optical communication," *J. Lightw. Technol.*, vol. 38, no. 2, pp. 421–431, 2020.
[7] H. M. Oubei *et al.*, "Light based underwater wireless communications," *Japanese J. Appl. Phys.*, vol. 57, no. 8S2, 2018, Art. no. 08PA06.
[8] J. Xu, "Underwater wireless optical communication: Why, what, and how?" *Chin. Opt. Lett.*, vol. 17, no. 10, 2019, Art. no. 100007.
[9] Z. Liu *et al.*, "Micro-light-emitting diodes with quantum dots in display technology," *Light: Sci. Appl.*, vol. 9, no. 1, pp. 1–23, 2020.
[10] P. Tian *et al.*, "High-speed underwater optical wireless communication using a blue gan-based micro-led," *Opt. Exp.*, vol. 25, no. 2, pp. 1193–1201, 2017.
[11] X. Liu *et al.*, "34.5 m underwater optical wireless communication with 2.70 Gbps data rate based on a green laser diode with nrz-ook modulation," *Opt. Exp.*, vol. 25, no. 22, pp. 27937–27947, 2017.
[12] J. Wang, C. Lu, S. Li, and Z. Xu, "100 m/500 mbps underwater optical wireless communication using an nrz-ook modulated 520 nm laser diode," *Opt. Exp.*, vol. 27, no. 9, pp. 12 171–12 181, 2019.
[13] C. Fei *et al.*, "16.6 Gbps data rate for underwater wireless optical transmission with single laser diode achieved with discrete multi-tone and post nonlinear equalization," *Opt. Exp.*, vol. 26, no. 26, pp. 34060–34069, 2018.
[14] H. M. Oubei, R. T. ElAfandy, K.-H. Park, T. K. Ng, M.-S. Alouini, and B. S. Ooi, "Performance evaluation of underwater wireless optical communications links in the presence of different air bubble populations," *IEEE Photon. J.*, vol. 9, no. 2, 2017, Art. no. 7903009.
[15] P. Tian *et al.*, "Absorption and scattering effects of maalox, chlorophyll, and sea salt on a micro-led-based underwater wireless optical communication," *Chin. Opt. Lett.*, vol. 17, no. 10, 2019, Art. no. 100010.
[16] D. Chen, J. Wang, S. Li, and Z. Xu, "Effects of air bubbles on underwater optical wireless communication," *Chin. Opt. Lett.*, vol. 17, no. 10, 2019, Art. no. 100008.
[17] M. V. Jamali, F. Akhoundi, and J. A. Salehi, "Performance characterization of relay-assisted wireless optical cdma networks in turbulent underwater channel," *IEEE Trans. Wireless Commun.*, vol. 15, no. 6, pp. 4104–4116, Jun. 2016.
[18] W. Liu, Z. Xu, and L. Yang, "Simo detection schemes for underwater optical wireless communication under turbulence," *Photon. Res.*, vol. 3, no. 3, pp. 48–53, 2015.
[19] Z. Vali, A. Gholami, Z. Ghassemlooy, M. Omoomi, and D. G. Michelson, "Experimental study of the turbulence effect on underwater optical wireless communications," *Appl. Opt.*, vol. 57, no. 28, pp. 8314–8319, 2018.
[20] F. Hanson and M. Lasher, "Effects of underwater turbulence on laser beam propagation and coupling into single-mode optical fiber," *Appl. Opt.*, vol. 49, no. 16, pp. 3224–3230, 2010.
[21] M. Sait *et al.*, "The effect of turbulence on NLOS underwater wireless optical communication channels," *Chin. Opt. Lett.*, vol. 17, no. 10, 2019, Art. no. 100013.
[22] M. Lewis *et al.*, "Characteristics of the velocity profile at tidal-stream energy sites," *Renewable Energy*, vol. 114, pp. 258–272, 2017.
[23] C. Rumbolz *et al.*, "Development of AlInGaN based blue-violet lasers on GaN and SiC substrates," *Physica Status Solidi (a)*, vol. 203, no. 7, pp. 1792–1796, 2006.
[24] X. Yi, Z. Li, and Z. Liu, "Underwater optical communication performance for laser beam propagation through weak oceanic turbulence," *Appl. Opt.*, vol. 54, no. 6, pp. 1273–1278, 2015.
[25] X. Luan, P. Yue, and X. Yi, "Scintillation index of an optical wave propagating through moderate-to-strong oceanic turbulence," *JOSA A*, vol. 36, no. 12, pp. 2048–2059, 2019.
[26] Y. Ata and Y. Baykal, "Scintillations of optical plane and spherical waves in underwater turbulence," *JOSA A*, vol. 31, no. 7, pp. 1552–1556, 2014.
[27] E. Zedini, H. M. Oubei, A. Kammoun, M. Hamdi, B. S. Ooi, and M.-S. Alouini, "Unified statistical channel model for turbulence-induced fading in underwater wireless optical communication systems," *IEEE Trans. Commun.*, vol. 67, no. 4, pp. 2893–2907, Apr. 2019.
[28] H. M. Oubei *et al.*, "Simple statistical channel model for weak temperature-induced turbulence in underwater wireless optical communication systems," *Opt. Lett.*, vol. 42, no. 13, pp. 2455–2458, 2017.